Study of Deposition of Al_2O_3 Nanolayers by Atomic Layer Deposition on the Structured ITO Films

© L.K. Markov[1], A.S. Pavluchenko[1], I.P. Smirnova[1], M.V. Mesh[2], D.S. Kolokolov[2], A.P. Pushkarev[3]

[1] Ioffe Institute,
194021 St. Petersburg, Russia
[2] Koltsov's Design Bureau,
198097 St. Petersburg, Russia
[3] ITMO University,
197101 St. Petersburg, Russia

E-mail: l.markov@mail.ioffe.ru

Received April 8, 2022
Revised May 5, 2022
Accepted June 2, 2022

In this work, the antireflective nanostructured ITO/Al_2O_3 coatings that have a gradient of the effective refractive index in the direction perpendicular to the substrate plane have been studied. The coatings were obtained by the atomic layer deposition (ALD) of aluminum oxide on the structured ITO films. The transmission electron microscopy showed that the deposited nanosized aluminum oxide layer was of good quality and uniformly covered the ITO whiskers. As shown in experiments, the thickness of the resulting Al_2O_3 layer is affected by the thickness and, hence, by the degree of surface roughness of the initial ITO film. The resulting thicknesses can be several times lower than that planned in the experiment, based both on the calculations of the parameters of the ALD process and on the direct measurements of the aluminum oxide deposition rate for unstructured ITO films. A possible reason that affects the growth rate of $A1O_3$ layers in nanostructured ITO films is a strong increase in the surface area of the ITO film during its structuring. So, the transmission and scanning microscopy data for a 700 nm-thick structured ITO film have shown that its surface area is more than 20 times greater than that of a smooth film.

Keywords: Indium tin oxide, aluminum oxide, atomic layer deposition, antireflective coatings, deposition rate.

DOI: 10.21883/SC.2022.08.54122.9856

1. Introduction

The antireflective coatings reducing the radiation losses when passing it through the interface between the two media with different refraction indices can substantially improve the operation characteristics of the instruments designed with optical elements. At the same time, such coating are designed both for the visible and infrared ranges of the spectrum.

As the technology of fabricating the optical coating is developed, there is distinctly the following trend: the multilayer non-structured films with the various refraction indices using the structural interference for reduction of the light losses give way to the structured coatings [1–4].

It is known that the refraction index of the substrate-medium interface can be reduced by applying to the substrate the heterogeneous layer with the refraction index smoothly changing within the refraction indices of its limiting media [5]. No contrast in the refraction indices of the film with the external media at the both film interfaces effectively minimizes light reflection. At this, the so-called gradient films are used within a wide range of the wavelengths of radiation propagating in various directions. The media with a various profile of the refraction index is theoretically studied in the study [6].

The gradient films can be fabricated by various methods, which are mainly reduced to designing the film consisting in the two components with the different value of the refraction index. If the particle sizes are significantly smaller than the radiation wavelength, the medium can be attributed with some effective refraction index determined by the percent content of the components as included in the coating. By changing the ratio of the components with the increase in the distance from one film interface and approaching another, correspondingly, we obtain the medium with a gradient of the effective refraction index. The task to fabricate the gradient coating effectively operating at the interface of the two media is reduced to searching the materials and methods of their common application in order to ensure smooth change of the effective refraction index within the refraction indices of the contacting media. The successful attempts to implement this approach applied for the various combinations of the materials can be found, for example, in the studies [7–10].

The gradient of the refraction index can be obtained for the single-component medium, in which the density of the material changes continuously. For this, the coating structure is provided with a various number of cavities. The methods of production of these media include, for example, application of the material at inclined incidence [11], anisotropic etching of the materials [12,13], anisotropic growth of nanosized filament crystals [14–17]. The methods of fabricating the antireflective coatings are reviewed in the

study [18], and the use of the gradient coatings in the nature is examined in papers [19,20].

Due to wide distribution of the means of visualization and data input (displays, touchscreens) as well as semiconductor light sources and photodetectors, the recent time has demanded the coatings which have good optical properties and are capable of simultaneously conducting the electric current for energizing or deenergizing an instrument cell. The study [21] has discussed the method of applying the coating of the Al_2O_3 thin layer for protection of the nanosized filaments of the antireflective films based on ITO. These films combine good optical properties with electric conductivity and can be used as transparent conductive coatings in a wide class of up-to-date instruments. However, due to the fact that these films have an extremely developed surface, the application of a chemically-resistant transparent protective layer can prevent their degradation caused by environmental factors. The study [21] has demonstrated that the atomic layer deposition (ALD) could form nanosized layers enveloping the filament crystals, from which the structured ITO film is composed of. This method consists in deposition of thin films from the gas phase and can be used to deposit the layers onto the surface of any development degree with an accuracy equal to the thickness of a monoatomic layer. It is especially important in terms of fabrication of the antireflective coating, since the excessive amount of the deposited material can change the density of the substance distribution in the film and, therefore, degrade its optical properties. As it has been shown in the study [21], the tryout of the thicknesses of the applied protective coating can keep a gradient nature of the refraction index inherent to the initial ITO film. The present study is dedicated to features of deposition of the Al_2O_3 protective coating on the developed surfaces of the ITO nanostructured films.

2. Experimental results and discussion

The nanostructured-ITO layer has been deposited by electron-beam evaporation using the combination deposition system produced by the Torr company (USA). The substrate (mounting slides of the 1.2-mm thickness) was pre-heated in a chamber to the temperature of 450°C. The thickness of the deposited ITO films evaporated in this study was 700 nm. Fig. 1 exemplifies it with the image of cleavage of one of the obtained films as obtained using the scanning electron microscope (SEM).

The atomic layer deposition of the Al_2O_3 layers was carried out using the Picosun P-300B, produced by „Picosun Oy“ (Finland). The deposition was performed by alternation of puffed agents (TMA (trimethylaluminum) + H_2O). The puffing time was 0.1 s, while the purging time was 3 s for TMA and 5 s for water. The specially-purified nitrogen was used a carrier gas. The thickness of the deposited layer was calculated based on the number of the process cycles performed.

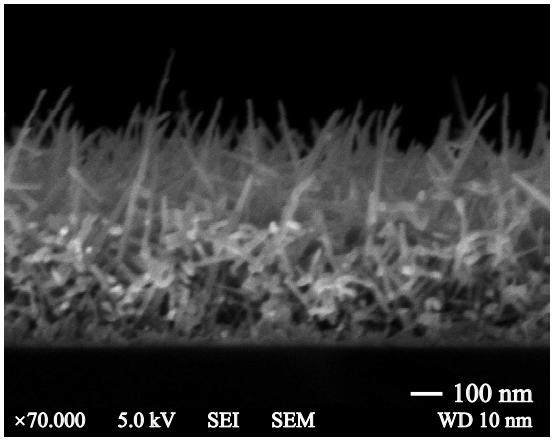

Figure 1. SEM-image of the ITO film.

The transmission and reflection spectra of the samples were examined using an Optronic Laboratories OL 770 spectroradiometer. The radiation was incident onto the samples from the film side normally to the surface.

The details of the technology of obtaining the nanostructured ITO films can be found in the study [22], while the details of the atomic layer deposition of the Al_2O_3 layers are described in the study [21]. Let us recall that as per the data of the scanning electron microscopy, for uniform deposition of a nanometer layer of the insulator along the entire length of the ITO filaments in the structured coating of the thickness of ~ 700 nm, it is required to perform the process at which the layer of 20-nm thickness will be deposited to the smooth non-structured surface. During the present study, these samples were studied by the methods of transmission electron microscopy (TEM). It is seen from Fig. 2 (which shows the image of the fragments of the filament ITO crystals covered with an insulating layer) that all the crystals are covered with a uniform Al_2O_3 layer of good quality. The thickness of the ITO filaments is ~ 15 nm, while the layer thickness of aluminium oxide can be estimated to be $7-8$ nm, which differs from the planned thickness of the coating, which is obtained based on the number of the process cycles performed and has been previously confirmed when calibrating the processes of deposition of the Al_2O_3 layers to the non-structured surfaces of the different materials for the plant used in the experiments.

In order to check the special features of deposition of the thin Al_2O_3 layers directly on the ITO material by the magnetron sputtering, the non-structured layer of the 200-nm thickness has been obtained (the amount of the ITO material in this film is equal to the amount of the material in the 700-nm structured film examined in the present paper). In the same process with the sample of the structured ITO, the layer of aluminium oxide with the design thickness of 20 nm was deposited on it at the temperature of 175°C. The cleavage of the obtained coating was studied by the scanning electron microscopy (Fig. 3). Despite the

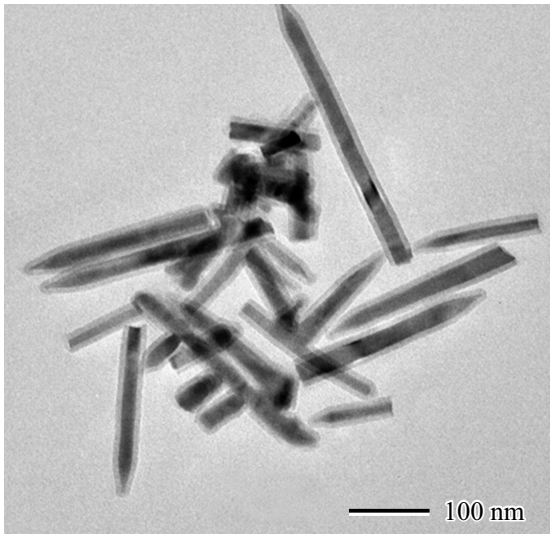

Figure 2. TEM-image of the filament ITO crystals covered with the Al_2O_3 layer.

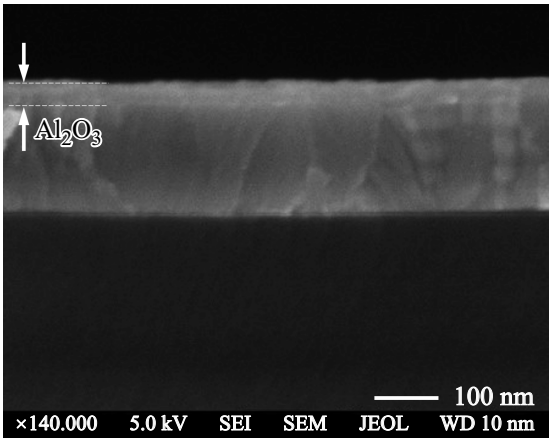

Figure 3. SEM-image of the Al_2O_3 layer on the surface of the non-structured ITO film.

insignificant contrast in the image of the ITO materials and Al_2O_3, the figure distinctly shows the interface between the two materials. The thickness of the obtained coating of the dielectric is close to 20 nm as expected.

Thus, we can say that despite the fact that at least the fragments of the filament crystals, which are located at the external film interface, are well accessible for agent gases, the deposition rate of the insulating coating is significantly (in 2.5 times) less than the growth rate on the non-structured ITO film. Let us note that we have noticed this fact for the first time when investigating the nature of deposition of the Al_2O_3 layer on the ITO structured films with the various thickness [21]. It has been turned out in the experiments that in order to uniformly cover the entire surface of the filament crystals of the ITO film of the 160-nm thickness, it is sufficient to perform the number of the ALD cycles in two times less than for the film of the 700-nm thickness.

One of the explanations of the observed dependence of the deposition rate of the Al_2O_3 layer on the development degree of the ITO material surface can be the significant increase in the surface area in structuring the material, which can be substantial taking into account a limited time of puffing and purging in the ALD cycle. Let us try to quantitatively evaluate the enlargement of the surface of our examined ITO films in comparison with the non-structured film. It is known (see [16]) that the structured-ITO films obtained by electron evaporation to the hot substrate have the following structure (Fig. 1): just on the substrate surface there is a quite dense nucleation layer of the thickness of 25–50 nm (depending on the film thickness). The layer consists of material grains and has a density of 0.8 of the density of the non-structured ITO material. The filament crystals, which start growing from the surface of the nucleation layer, occupy the whole remaining volume of the film to its external interfaces. In the real film, they have a various length and are non-ideally parallel to each other, thereby providing for a gradient of the material in a direction perpendicular to the substrate plane. The film is schematically shown on Fig. 4, *a*. In order to evaluate the specific surface of the structured films, we present the filament crystals as an ensemble of the parallel cylinders (Fig. 4, *b*). The diameter of the cylinders — 15 nm, (as per the data of Fig. 2), while their length for evaluating the surface increment during structuring is of no importance. But, for convenience, we accept it to be equal to the thickness of the whole film minus the thickness of the nucleation layer. It is just only necessary to satisfy a condition consisting in that the weight of the material per the filament crystals complies with the experimental data. Let us recall that as per the data of the study [21], the structured films of the thickness 160 and 700 nm were equivalent in weight to the non-structured films of the thickness of 50 and 200 nm, respectively. Thus, finding the volume of one cylinder of the filament crystal, we can evaluate the number of the cylinders per a unit substrate surface, and by calculating the side surface of each crystal, in the following action we can find the total surface of all the side crystals per the unit substrate surface. And this value will correspond to the increment of the surface of the material obtained as a result of structuring.

The calculation based on the above-listed considerations shows that for the film of the thickness of 700 nm the surface increases in 22.3 times, so does the film of the thickness of 160 nm in 5 times (the thickness of the nucleation layer for these films is accepted to be 50 and 25 nm, respectively).

Let us note that in the evaluation used we downgrade the obtained value by neglecting the fact that the nucleation layer of the real film is not flat, as described by us in our model (see Fig. 1). Moreover, as we see from Fig. 2, in reality the filament crystals have conical not flat tips. If in a simplified form, we consider that the surface of

the nucleation layer consists in hemispheres of the grains, and the filament crystal have non-flat tips, then only these two factors already increase the surface in comparison with the smooth film even without taking into account the side surface of the cylinders.

Another special feature of deposition of the thin Al_2O_3 layer to the surfaces of the ITO nanostructured films was the dependence of behavior of deposition of the protective coating on the process temperature. The study [21] has noticed that the ALD process at the temperature of 300°C is associated with the increased integral absorption in the field after application of the protection to the structured ITO films. The reduction of the process temperature to 175°C decreases the absorption in the coating to the values observed in the unprotected film. At the same time, as per the SEM diagnostics, all the filaments of the structured conductive coating turn out to be covered with the Al_2O_3 layer in the same way as at the process temperature of 300°C. In our assumption, the increased process temperatures can accelerate the diffusion of oxygen atoms from the filaments of the protective coating into the insulator film when it is growing. It is known that oxygen

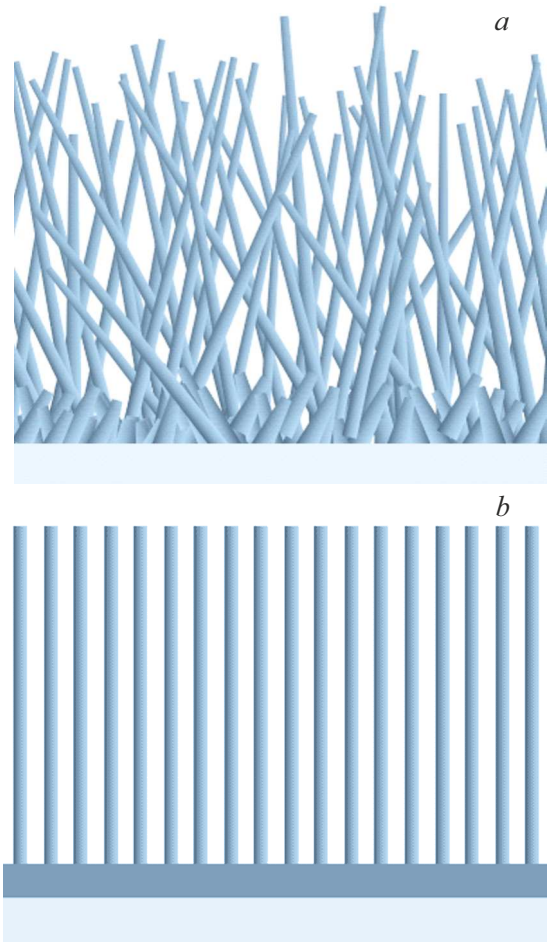

Figure 4. Schematic representation of the ITO nanostructured film: *a* — real view, *b* — used for evaluating the specific surface.

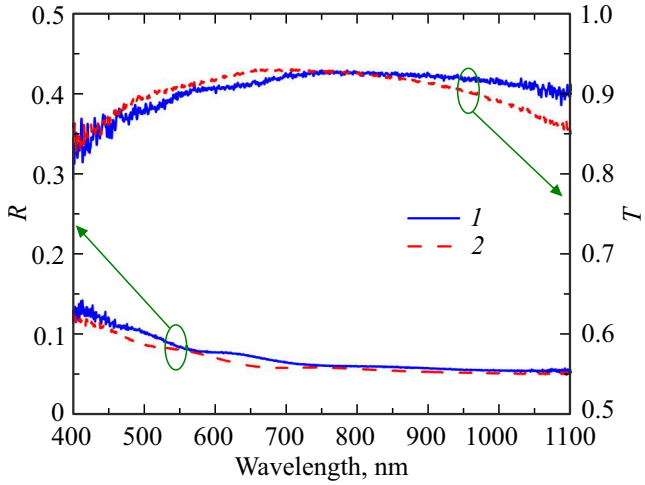

Figure 5. Transmission and reflection spectra of the samples obtained at the ALD temperature 50°C (the curves *1*) and 175°C (the curves *2*).

depletion of the ITO material results in additional light absorption therein. In order to investigate the properties of the coating obtained at the various temperatures of deposition of the protective layer, the process was conducted at the temperature of 50°C. The spectra of reflection and absorption of the obtained coating and the coating with the ALD process temperature of 175°C are shown on Fig. 5. As per the figure, the optical characteristics of both the coatings are close to each other. But, it may be noted that the reduction of the ALD process temperature from 175 to 50°C slightly increases the sample reflection within the whole range of the wavelengths, while, respectively, the transmittance of the sample is insignificantly decreased within the visible range of the wavelengths. The observed drop of the transmittance of the sample obtained at the ALD process temperature of 175°C is apparently related to the additional absorption, which occurs, as we discussed above, in the ITO filaments due to the diffusion of oxygen out of them when depositing the protective layer. Thus, despite the fact that the ALD process temperature of 175°C significantly reduces light losses in the coating in comparison with the temperature of 300°C, it is possible to try minimizing them in the IR range.

However, the structure of the sample obtained at the ALD process temperature of 50°C was studied by means of the scanning electron microscopy (Fig. 6) to show that at this temperature the Al_2O_3 layer was deposited not along the entire length of the nanofilaments of the ITO structured layer. This factor seems to be a reason of increase in the reflection from this coating in comparison with the coating obtained at the increased ALD temperatures. Thus, nonuniform coating of the filaments results in the distortion of the gradient of the density of the substance in the film and, respectively, the effective refraction index, thereby reducing the antireflectivity of the coating.

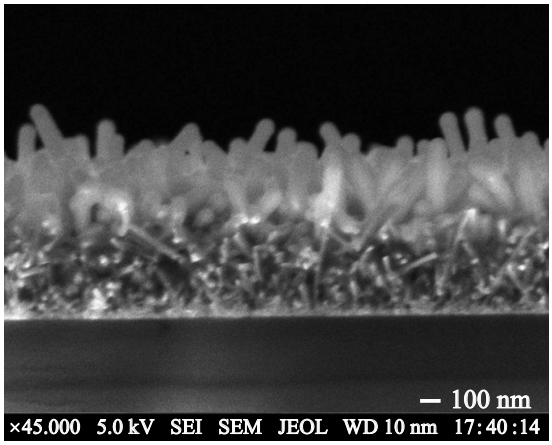

Figure 6. SEM image of the coating deposited at the ALD process temperature of 50°C.

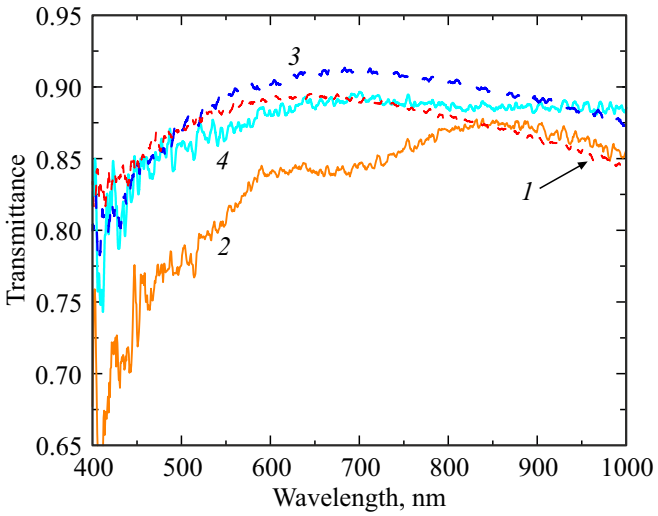

Figure 7. Transmission spectra of the samples before and after the test in the moisture chamber: *1* — the sample of the nanostructured ITO without the protective coating before the tests, *2* — the sample of the nanostructured ITO without the protective coating after the tests, *3* — the sample of the nanostructured ITO with the protective coating before the tests, *4* — the sample of the nanostructured ITO with the protective coating after the tests. (A color version of the figure is provided in the online version of the paper).

The very fact of deposition of the Al_2O_3 layer only on the surface areas of the structured ITO coating at the temperature of 50°C is quite interesting. Since at the process temperature of 175°C this special feature is absent, it can be suggested that despite the fact that in the ITO structured film all the surface of the nanofilaments seems to be open for the gaseous medium of the agents, with this surface geometry their diffusion in the low layers of the film can be difficult. Correspondingly, the increase in the temperature contributes to acceleration of the diffusion processes and uniform burial of the filaments across the coating thickness.

In order to evaluate the influence of the Al_2O_3 protective layer on the operation characteristics of the ITO nanostructured films, the samples were manufactured both with and without the coating.

After measurement of the optical characteristics of the produced samples, they were placed in the moisture chamber MC 5/100-250 TVO and subjected to the following impact of the increased humidity as per GOST RB 20.57.306 (the accelerated tests for the category O): the duration of the first part of the cycle was 12 hours, the temperature — 55°C, the humidity— 93%, the duration of the second part of the cycle was 12 hours, the temperature — 25°C, the humidity — 95%. Totally, there were 9 cycles.

Fig. 7 shows the transmission spectra of the samples taken before and after the tests performed. As per the data obtained, the transmittance of the films without the Al_2O_3 protective coating is degrading much more heavily (the curves *1* and *2*) than with the protective coating (the curves *3* and *4*).

3. Conclusion

Thus, studying the antireflective ITO nanostructured/Al_2O_3 coating by means of the transmission electron microscopy has shown that the transmission electron microscopy forms the layer of good quality, evenly enveloping the filament ITO crystals. However, the thickness of the obtained layer of aluminum oxide is in several times thinner than the planned calculation thickness of the layer in the experiment. At the same time, the model experiment for deposition of the Al_2O_3 layer to the surfaces of the ITO non-structured film has shown coincidence of the deposited thickness with the calculated one. The surface area of the structured ITO was evaluated based on the data of the transmission electron microscopy and the scanning electron microscopy to show that in structuring the surface area increases in more than 20 times in comparison with the area of the smooth surface. It might be the main factor affecting the growth rate of the Al_2O_3 layer within the ITO nanostructured films. The surface area for the structured film of the smaller thickness is evaluated a lesser increment of the area during structuring, thereby complying with the experiment results, in which there is the intermediate growth rate between the smooth one and the thicker one.

The structure of the sample obtained at the reduced ALD temperature (50°C) was studied by means of the scanning electron microscopy to show that at this temperature the Al_2O_3 layer was deposited not along the entire length of the nanofilaments of the ITO structured layer, but only at the external parts of the filaments, which can probably be explained by limiting the diffusion processes with the reduction of the temperature.

Conflict of interest

The authors declare that they have no conflict of interest.

References

[1] H. Wang, F. Zhang, C. Wang, J. Duan. Opt. Laser Techn., **149**, 107931 (2022).
[2] N. Cherupurakal, M.S. Mozumder, A.H.I. Mourad, S. Lalwani. Renew. Sustain. Energy Rev., **151**, 111538 (2021).
[3] H. Sun, J. Liu, C. Zhou, W. Yang, H. Liu, X. Zhang, Z. Li, B. Zhang, W. Jie, Y. Xu. ACS Appl. Mater. Interfaces, **13**, 16997 (2021).
[4] A. Jacobo-Marín, M. Rueda, J.J. Hernández, I. Navarro-Baena, M.A. Monclús, J.M. Molina-Aldareguia, I. Rodríguez. Sci. Rep., **11**, 1 (2021).
[5] J.W.S. Rayleigh. Proc. London Math. Soc., **11**, 51 (1880).
[6] J.A. Dobrowolski, D. Poitras, P. Ma, H. Vakil, M. Acree. Appl. Optics, **41**, 3075 (2002).
[7] J.-Y. Cho, K.-J. Byeon, H. Lee. Optics Lett., **36**, 3203 (2011).
[8] J.K. Kim, A. N. Noemaun, F.W. Mont, D. Meyaard, E.F. Schubert, D.J. Poxson, H. Kim, C. Sone, Y. Park. Appl. Phys. Lett., **93**, 221111 (2008).
[9] P.G. O'Brien, D.P. Puzzo, A. Chutinan, L.D. Bonifacio, G.A. Ozin, N.P. Kherani. Adv. Mater., **22**, 611 (2010).
[10] P. G. O'Brien, Y. Yang, A. Chutinan, P. Mahtani, K. Leong, D.P. Puzzo, L.D. Bonifacio, C.W. Lin, G.A. Ozin, N.P. Kherani. Sol. Energy Mater. Sol. Cells, **102**, 173 (2012).
[11] J.K. Kim, S. Chhajed, M.F. Schubert, E.F. Schubert, A.J. Fischer, M.H. Crawford, J. Cho, H. Kim, C. Sone. Adv. Mater., **20**, 801 (2008).
[12] T. Aytug, A.R. Lupini, G.E. Jellison, P.C. Joshi, I.H. Ivanov, T. Liu, P. Wang, R. Menon, R.M. Trejo, E. Lara-Curzio, S.R. Hunter, J.T. Simpson, M.P. Paranthaman, D.K. Christen. J. Mater. Chem. C, **3**, 5440 (2015).
[13] L.K. Markov, I.P. Smirnova, M.V. Kukushkin, A.S. Pavlyuchenko. FTP, **6**, 564 (2020) (in Russian).
[14] M.J. Park, C.U. Kim, S.B. Kang, S.H. Won, J.S. Kwak, C.-M. Kim, K.J. Choi. Adv. Opt. Mater., **5**, 1600684 (2017).
[15] Z. Gong, Q. Li, Y. Li, H. Xiong, H. Liu, S. Wang, Y. Zhang, M. Guo, F. Yun. Appl. Phys. Express, **9**, 082102 (2016).
[16] L.K. Markov, A.S. Pavlyuchenko, I.P. Smirnova, S.I. Pavlov. FTP, **52**, 1228 (2018) (in Russian).
[17] L.K. Markov, A.S. Pavlyuchenko, I.P. Smirnova. FTP, **53**, 181 (2019) (in Russian).
[18] Z.W. Han, Z. Wang, X.M. Feng, B. Li, Z.Z. Mu, J.Q. Zhang, S.C. Niu, L.Q. Ren. Biosurface and Biotribology, **2**, 137 (2016).
[19] M. Kryuchkov, J. Lehmann, J. Schaab, V. Cherepanov, A. Blagodatski, M. Fiebig, V.L. Katanaev. J. Nanobiotechnology, **15**, 61 (2017).
[20] M. Kryuchkov, O. Bilousov, J. Lehmann, M. Fiebig, V.L. Katanaev. Nature, **585**, 383 (2020).
[21] L.K. Markov, A.S. Pavlyuchenko, I.P. Smirnova, M.V. Mesh, D.S. Kolokolov. FTP, **55**, 365 (2021) (in Russian).
[22] L.K. Markov, I.P. Smirnova, A.S. Pavlyuchenko, M.V. Kukushkin, D.A. Zakgeim, S.I. Pavlov. FTP **50**, 1001 (2016) (in Russian).